Northeast Journal of Complex Systems (NEJCS)

Volume 3
Number 1 *Special Issue: NERCCS 2021 Papers*

Article 3

March 2021

Network-Based Analysis of Early Pandemic Mitigation Strategies: Solutions, and Future Directions

Pegah Hozhabrierdi
Syracuse University, phozhabr@syr.edu

Raymond Zhu
Syracuse University, rzhu09@syr.edu

Maduakolam Onyewu
Syracuse University, monyewu@syr.edu

Sucheta Soundarajan
Syracuse University, susounda@syr.edu

Recommended Citation

Hozhabrierdi, Pegah; Zhu, Raymond; Onyewu, Maduakolam; and Soundarajan, Sucheta (2021) "Network-Based Analysis of Early Pandemic Mitigation Strategies: Solutions, and Future Directions," *Northeast Journal of Complex Systems (NEJCS)*: Vol. 3 : No. 1 , Article 3.
DOI: 10.22191/nejcs/vol3/iss1/3
Available at: https://orb.binghamton.edu/nejcs/vol3/iss1/3

Network-Based Analysis of Early Pandemic Mitigation Strategies: Solutions, and Future Directions

Pegah Hozhabrierdi[†], Raymond Zhu[*], Maduakolam Onyewu[*], and Sucheta Soundarajan

Department of Electrical Engineering and Computer Science
Syracuse University, Syracuse, NY
{phozhabr,rzhu09,monyewu,susounda}@syr.edu

Abstract

Despite the large amount of literature on mitigation strategies for pandemic spread, in practice, we are still limited by naïve strategies, such as lockdowns, that are not effective in controlling the spread of the disease in long term. One major reason behind adopting basic strategies in real-world settings is that, in the early stages of a pandemic, we lack knowledge of the behavior of a disease, and so cannot tailor a more sophisticated response. In this study, we design different mitigation strategies for early stages of a pandemic and perform a comprehensive analysis among them. We then propose a novel community-based isolation method and show its efficacy in reducing the speed of the spread by a large margin as compared to current methods. We also show that the test-trace-isolation strategy can outperform lockdown and random test-trace in reducing the economic impact and spread of the disease if combined with k-hop neighborhood ranking. The novelty of our work lies in using network structural properties (local and global) to design a strategy for the early stages of a pandemic. Our results encourage further investigation into community-based mitigation strategies and shed more light on the differences between current methods of choice in practical setting.

1 Introduction

In response to the COVID-19 pandemic, governments across the world have attempted a variety of strategies to mitigate the spread of disease, including lockdowns, contact tracing, and others. However, there has been little analysis on the

[†]Corresponding author
[*]Equal contribution

relative merits of such strategies; and because these strategies have negative effects on the economy and the morale of the people, it is critically important to understand their efficacy. Although this work is inspired by the COVID-19 pandemic, our analysis can apply to any contagious disease. Because the response to a pandemic depends on whether it is in the early stages (no vaccination available) or later stages (vaccination available), we focus on early pandemic mitigation strategies in correspondence with the COVID-19 situation.

In this work, we analyze variants of the pandemic mitigation strategies practiced in the real world – e.g. lockdown and test-trace-isolate – from a network perspective. Inspired by the new psychology findings on the correlation between community membership and pandemic response [1, 2, 3], we also offer a community-based mitigation strategy and demonstrate its efficacy in comparison. To the best of our knowledge, we are the first to offer a network-based comparison of practical mitigation strategies in the early stages of a pandemic. To evaluate each strategy, unlike the majority of related work in this field, we consider both the speed of spread and economic impact as cost factors. For example, a mitigation strategy such as a total lockdown might have the best performance in terms of controlling the spread of disease if prolonged for long enough time until the discovery of the vaccine. However, the devastating economic impacts of such a decision makes this strategy inefficient in the real world. On the other hand, the "Do Nothing" strategy, which relies on herd immunity (see Section 3), results in less economic impact (at least in the early stages), but does nothing about the spread of the disease. An ideal mitigation strategy should offer a trade-off between these two losses. We allocate a budget to each strategy to count for the economic impact and report both the spread and budget spent for each strategy simulation.

To ensure that our results are generalizable to other contagious diseases, we enforce only general assumptions about the nature of the disease and cost of battling the spread (see Section 2). We use the SIRD epidemic model for our simulations and only consider the budget spent on isolation strategies. We validate each strategy on a set of 10 real-world social networks (see Section 4.2). To have a close approximation of human-human contact behavior, these networks are chosen based on the method of data collection and the meaning of connections between two individuals. We also consider a set of online social networks that are frequently used in the disease spread literature [4, 5, 6] and, in some cases, have been shown to give a close-enough approximation of real-world social networks [5]. Our results show the superiority of the test-trace-isolation strategy if combined with k-hop neighborhood ranking (specifically for k = 1). We also confirm the theoretical results from psychology studies on the impact of community membership in reducing the spread of the disease and show the further direction in adopting such strategies.

https://orb.binghamton.edu/nejcs/vol3/iss1/3
DOI: 10.22191/nejcs/vol3/iss1/3

2 Problem Statement

We model the population as a simple undirected graph $G(V, E)$, where individuals are represented by nodes (V) and connections between them (E) represent physical contact. We use undirected edges due to the nature of physical contact, for which a directed relationship does not bear any meaning. We also consider unweighted and un-attributed graphs, as attribute information is not easy to gather in a real-world setting and in the practical strategies discussed below. However, our simulations can easily be extended to attributed or weighted graphs. For example, the strength of an edge can be considered as the frequency or length of the contact, where a higher value increases the probability of infection spread. In the following discussion, we discuss different models of disease spread and the reasons behind our choice of the SIRD model. We will also discuss our method of extending the model to count for the economic impact.

2.1 Viral Spread Modeling

Previous work on mathematical modeling of viral spread can be grouped into two categories of (1) general spread models and (2) virus-specific spread models. The former includes famous models such as SIR, SIRD, SIS, SIER, and SIRS [7, 8, 9]. The virus-specific models have been proposed for viruses observed in real world and consider the specific properties of a certain virus into the modeling of the spread [10, 11, 12]. The focus of our study is on the effectiveness of different mitigation strategies for an unknown pandemic scenario (i.e., a pandemic whose specific behavior and potential remedies are unknown). It is known that battling a new pandemic heavily relies on adopting a proper mitigation strategy in its early stages [13]. In these early stages, our knowledge of the nature of the virus is very limited, and the virus-specific strategies require prior knowledge gained from time-consuming clinical trials. Thus, the general models with little to no conditions on virus-specific behavior are more practically applicable in the early stages of a pandemic. For our study, we choose the SIRD model due to its minimal assumptions on the nature of a fatal spread, which is explained below.

2.2 SIRD Epidemic Model

Given a *closed* community in which the population is fixed (no birth, no migration, and no death due to causes irrelevant to the disease under study), the SIRD model assumes four possible states for each individual in the community at each timestamp: Suceptible (never contaminated by the virus), Infectious (contaminated and can spread the virus), Recovered (recovered from contamination and can no longer

spread the virus), and Dead (due to infection). The possible transition between states and their respective probabilities are depicted in figure 1.

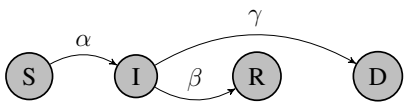

Figure 1: SIRD state transitions. Parameters α, β, and γ indicate infection, recovery, and mortality rate respectively.

The three parameters of this model are α, β, and γ that indicate infection, recovery, and mortality rate respectively. Their exact values used in our simulations are presented in Table 2 and discussed in Section 4. In Section 4.5, we discuss the choice of these hyperparameters and validate the robustness of our results for different values of α, β, and γ. We use a discrete-time SIRD model with discretization period of duration one day. Having initial values S_0, I_0, R_0, D_0 in a population of size N, the virus spread follows these laws of motion:

$$S_{t+1} = S_t - \alpha \frac{I_t S_t}{S_t + I_t} \tag{1}$$

$$I_{t+1} = I_t + \alpha \frac{I_t S_t}{S_t + I_t} - (\beta + \gamma) I_t \tag{2}$$

$$R_{t+1} = R_t + \beta I_t \tag{3}$$

$$D_{t+1} = D_t + \gamma I_t \tag{4}$$

We assume that no individual can stay in I state indefinitely. As such, every infectious individual can only stay infected for a certain amount of time (disease duration in Table 2) and transitions to R if not deceased or recovered already. Note that we do not consider any delay in the transitions.

2.3 Budget Allocation

The exact modeling of a pandemic's economic impact is a complicated problem and requires a comprehensive study on its own [14, 15, 16]. However, we still can introduce a simplified measure of cost for comparison between different mitigation strategies. As we try to minimize the number of isolated individuals while reducing the rate of spread, we have to compensate for the portion of the population that is under quarantine (either compulsorily or voluntarily) to make isolation practical and possible without threatening the well-being of families and individuals. We treat this compensation as a required budget for each isolation strategy. Ultimately, an

ideal isolation strategy should use a small compensation budget while minimizing the peak number of the infectious population over time. A smaller amount of budget spent also indicates isolated individuals, implying less possibility of economic impact due to work-force perturbation.

3 Mitigation Strategies

Two of the most important problems in the early stages of a pandemic are (1) the capacity of healthcare centers and (2) economic consequences [14, 15, 16, 17]. An optimal mitigation strategy seeks to reduce the occupancy of hospitals (lower the number of infected) while maintaining the productivity of the society to eliminate economic impacts. However, these two objectives often bear conflicting interests. So far, the strategies for lowering the number of infected individuals practiced in real-world setting have negatively affected the economic well-being of the society. A current example is the **Lockdown strategy** adopted by many countries (such as the USA, Spain, and Italy) in 2020 to mitigate the COVID-19 spread[1]. Interestingly, lockdown does not offer an optimal solution to either of the objectives above. First, lockdown leads to a *second wave* of spread and has to be implemented in several phases to be effective in lowering the burden on the healthcare system [18]. Second, it is shown (both in theory and practice) that lockdown strategy causes severe damages to the economy [17].

To trade-off between the need for isolation and economic prosperity, [17] suggests employing a **Test-Trace-Isolate strategy (TTI)**. This method puts the focus on the neighborhood of the individuals with positive test results (infected). According to [19], the countries who employed the TTI strategy against COVID-19 were able to combat the spread more successfully than those who followed *herd immunity*[2] or full containment (lockdown) strategy. This, however, mainly considers the medical benefits of the mitigation. The cost-effectiveness of TTI (economical aspect) heavily depends on its implementation [20]. For example, how do we choose whose neighborhood to trace? Is it the people who show symptoms or those who have tested positive? Furthermore, how many people in the candidate's neighborhood should we isolate and how big should the size of this neighborhood be? Tracing and isolating steps of TTI are costly and, if implemented in a naïve way, it can be less efficient than lockdown strategy. In this study, we examine three different strategies for TTI. These methods all use local neighborhood information. We con-

[1] `https://en.wikipedia.org/wiki/COVID-19_pandemic_lockdowns`

[2] Herd Immunity is an epidemiological concept and is defined as "the percentage of people with protective immunity needed in a population to stop the propagation of an infectious agent" [19]. This strategy, although seemingly giving an optimal solution to economic impact of the spread, results in a devastating death toll in the population.

sider random and centrality-based TTI with tracing radius up to k-hops away from the infected node (for $k \in \{1, 2\}$). The details of each method are discussed in Section 4. Note that due to small-world property of social networks, for k values higher than two, we capture almost all of whole network, which is counter-intuitive for TTI strategy.

In a pandemic, human behavior plays as important of a role as properties of the virus (if not a more important role) [1]. Such behavior is directly connected to psychological traits of individual's personality [2]. An interesting relevant observation is that shared community membership increases the speed of the spread [3]. Previous studies have shown there is a correlation between community structure and spread behavior (e.g., under certain community structure, the spread is slowed down or sped up) [21, 22]. In a recent study, [23] shows that community size and density play an important role in the predictability and controllablity of epidemic. These observations are used in immunization literature to leverage the community structure for optimizing the immunization plan. For example, in [24], authors propose a heuristic for finding potential community bridges and immunize them. In [25], several ranking methods based on the in/out degree of nodes in a community are proposed to choose a community for immunization.

The immunization is mainly done when enough information is available about the virus and it is possible to use time-consuming heuristics for finding the optimized set of nodes to immunize. Moreover, the immunization is not as costly as isolation strategies due to the prolonged nature of the latter.The target of our current study is to act in the early-stages and with limited to no knowledge on the nature of the disease. We tend to find a balance between lowering the cost and the peak of infection by using isolation strategies in the absence of vaccines/remedies. We argue that by considering the findings in the aforementioned studies, we can improve isolation-based mitigation strategies. As such, we propose a **Community-based Isolation strategy (CI)** and show its effectiveness in comparison to lockdown and TTI strategies. The results of CI are presented to show that using the community membership of individuals as an isolation strategy indeed reduces the speed of spread. At first glance, this method might not be as practical as lockdown or TTI, owing to the fact that community membership is only partially known and tracing the memberships can be even more costly that TTI (as shown in Section 4). However, the results of our experiments show that community-based isolation surpasses all other methods in reducing the spread of the disease without the disadvantage of a second wave. We argue that further approximation of community information and isolation of only bridge nodes (those who contribute the most to the spread from one community to the next) can improve the cost associated with CI strategy.

4 Experiments

In this section, we evaluate each of the baseline strategies against our proposed methods. We focus only on real-world data to consider the complex dynamics of the human-human interaction, which is not entirely captured in synthetic networks (e.g, stochastic block model, small-world model, etc.).

4.1 Assumptions

As mentioned before, for lockdown and TTI, we do not enforce any disease-specific information on the model. Additionally, we do not assume the presence of network structural data that are hard or impossible to obtain in real-world setting. For example, we do not assume that we have global information for nodes or edges (e.g. shortest path-based centralities, diameter of the network, or spectral properties). We only have the information on the neighborhood of each individual (as obtained through individual surveys in real world). It is noteworthy that we consider the neighborhood information to be incomplete and any new information added to our data will improve the result of the simulations.

For CI, we assume the community membership of individuals is known. In the real-world, the communities can be considered at different levels; from a club membership level up to county and state levels. Considering that not all of our datasets have ground-truth communities, we obtain membership through Louvain partitioning of the graph that maximizes the modularity.

4.2 Data

Recent studies show the importance of using real-world human-human interaction data to account for the influence of human behavior in the simulation of a spread [1]. We chose seven real-world datasets that have been collected based on physical human interaction/connections in real world. These datasets, although the best resource for real-world interactions, are generally small due to the cost of data collection. As such, many studies tend to use online social networks as approximate behavior of the users in physical world. [5] showed that online behavior approximation for some online networks such as Facebook is close to physical behavior. To both confirm their results for other online social networks and consider the result of our simulation on larger networks, we also consider an additional three larger datasets from online social networks. All of our 10 datasets are chosen based on the nature of their contact (edge meaning). These datasets and their general statistics

Data	Type	Edge Meaning	$\|V\|$	$\|E\|$	Avg. Deg.
Infectious (INF)	Human Interaction	Contact	410	2,765	13.49
Hyptertext2009 (HX9)	Human Interaction	Contact	113	2,196	38.87
Haggle (HAG)	Human Interaction	Contact	315	2,899	18.41
Adolescent Health (AH)	Human Social	Friendship	2,539	10,455	8.23
Residence Hall (RH)	Human Social	Friendship	217	1,839	16.95
Physicians (PHY)	Human Social	Trust	241	923	7.66
Jazz Musicians (JAZ)	Human Social	Collaboration	198	2,741	27.69
Pretty Good Privacy (PGP)	Online Contact	Interaction	10,680	24,316	4.55
Facebook NIPS (FBN)	Online Social	Friendship	2,888	2,981	2.06
Hamster Full (HAM)	Online Social	Friendship	2,426	16,630	13.71

Table 1: Contact datasets for spread simulation

are shown in Table 1. All datasets are publicly available in the Konect repository[3] [26].

4.3 Implementation of Mitigation Strategies

In this section, we briefly go over the implementation of each mitigation strategy mentioned in Section 3. The hyperparameters are the same among all strategies (such as quarantine compensation, duration of quarantine, duration of disease, and parameters α, β, γ). These hyperparameters are presented in Table 2. In all simulations, we start with only one infectious node chosen at random (i.e, $I_0 = 1$, $S_0 = |V| - 1$, $R_0 = D_0 = 0$, unless otherwise specified). For each model, we repeat the simulation for 100 different starting node and report the average among the 100 trials. Each round of simulation is run until there are no infected nodes left in the network. In each timestamp t_i, the number of infected, susceptible, and quarantined individuals are reported based on the networks status in t_i. The reported proportion of infected individuals is averaged over the timestamps in the simulation. The number of deceased and recovered individuals are reported cumulatively (from t_0 to t_i).

- **Do Nothing (DN)**: Although not exactly a mitigation strategy, DN can be used as the baseline to compare the performance of other methods against it. It is a simple SIRD model (Equation 1 – 4) that reaches the peak of infection quickly and fades away quickly as well (due to herd immunity).
- **Lockdown**: The duration of the lockdown is fixed at 14 days, and it starts after the detection of the first infectious sample. We randomly choose 90% of

[3] At the time of writing this paper, we noticed Konect project is discontinued. For obtaining our dataset, please email the corresponding author.

Hyperparameter	Value
Probability of infection (α)	0.2
Probability of recovery (β)	0.08
Probability of death (γ)	0.04
Simulation unit of time	1 day
Disease duration	7 days
Quarantine duration	14 days
Daily quarantine compensation (Compulsory Isolation)	\$100
Daily quarantine compensation (Volunteer isolation)	\$50
Volunteer quarantine probability	0.5

Table 2: Hyperparameters chosen for all mitigation strategies when applicable.

the population for lockdown and compensate all of them according to *Daily quarantine compensation (compulsory isolation)* in Table 2. After the lockdown is lifted, the disease spreads according to the SIRD model and we expect the same peak as in DN but shifted over time. Note that this model adds a new state *Q*, for *Quarantined*, to Figure 1 with $Q_0 = 0.9|V|$, but does not change the equations.

- **TTI**:
  - *K-hop Ranking for* $k \in \{1, 2\}$: Prior to the simulation, each node is ranked according to the size of its k-hop neighborhood. For example, if the rank of a node is 16, it means this node, if infectious, can potentially contaminate 16 other individuals. In the tracing stage of TTI, we choose to forcibly isolate neighborhood of an infected node who have a ranking above 90 percentile of all rankings in the graph. We also choose the neighborhood with ranking above 80 percentile (and less than 90 percentile) as candidates to voluntarily quarantine themselves. Both of these groups (forced quarantine and volunteer quarantine) are compensated but with different amounts (see *Daily quarantine compensation* for compulsory and volunteer isolation in Table 2). We assume the candidates for volunteer isolation accept the offer 50% of the times. Note that both of these thresholds can be chosen via trial and error and do not require global information on the graph.
  - *Random Ranking*: In the tracing stage of TTI, we randomly choose candidates from the k-hop neighborhood ($k \in \{1, 2\}$) of an infected node to isolate. The isolated nodes are compensated as in lockdown.
- **CI**: We obtain community memberships through Louvain partitioning [27]. At each timestamp, we isolate an entire community if the portion of infected

nodes within the community is greater than a threshold, i.e. $\frac{I_c}{|V_c|} > T$ where $|V_c|$ is the population within community c and T is a hyperparameter. We report the results for $T \in \{0.1, 0.2, ..., 0.9\}$. The isolated members are compensated as in lockdown.

Note that the choice of parameters such as disease duration and quarantine duration does not affect our comparison between Lockdown and TTI strategies as this parameter is set equally for all of them. In Section 4.5 we show that our comparisons are also robust against the choice of α, β, and γ.

4.4 Results & Discussion

The results of the DN, Lockdown, and TTI strategies are shown in Figure 2. In this figure, the y axis depicts the average (and variance) of the infectious population normalized by the overall population. In all datasets, the best performance is achieved through the k-hop neighborhood strategy. In 7 out of 10 datasets, the 2-hop strategy achieves a better performance and, in most cases, it is very close to that of 1-hop. However, looking at the required budget in Figure 3, it is evident that the choice of 2-hop neighborhood comes with a greater cost, especially for HX9 dataset. To understand the reason behind enormous 2-hop budget for HX9, we need to look at the number of triangles in the network normalized by the maximum possible triangle count ($|V|(|V|-1)(|V|-2)$). In our dataset, HX9 has the highest value for normalized triangle count (10 times more than the next highest count). Due to this high clusterability of HX9, the 2-hop neighborhood captures the entirety of the network and, in practice, gives a less optimal result than lockdown or even DN strategy in terms of budget. The special case with HX9 dataset shows the limitation of choosing 2-hop over 1-hop neighborhoods of the infectious nodes. Considering this trade-off between cost and peak of infection, we can conclude that 1-hop TTI strategy is the best practical strategy among the rest in real-world scenarios.

As the results for CI-based isolation are threshold-dependent, we have shown its results separately in Figure 4 and 5 for various threshold values. CI, surprisingly, does a much better job at reducing the infectious peak than any of the other methods (compare Figure 4 with Figure 2). This confirms the suggestions from psychology literature that mitigation strategies based on community membership can result in a better control over the speed of the spread. However, the thresholding is very important for CI. As seen in Figure 5, for higher thresholds, CI generally comes with a much higher budget than TTI, and unlike the previous methods, surpasses the lockdown budget in many instances. However, keeping the threshold below 0.4 offers a considerable reduction in speed with a reasonable budget. On the other hand, we argue that our proposed CI strategy uses limited information and still performs

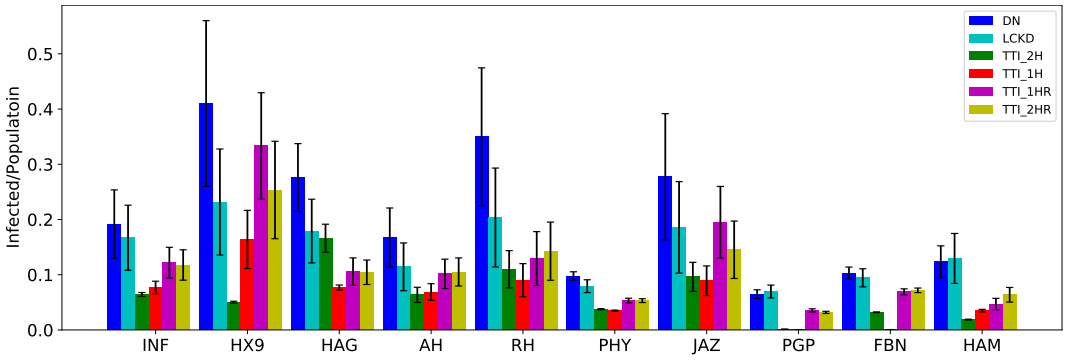

Figure 2: The average proportion of infected individuals over 100 trials of simulation and its variance for each mitigation strategy among our datasets. DN, LCKD, and TTI abbreviate *Do Nothing*, *Lockdown*, and *Test-Trace-Isolate* strategies. TTI suffixes: 1H and 2H represent k-hop ranking, 1HR and 2HR represent random ranking within k-hop neighborhood. Best viewed in color.

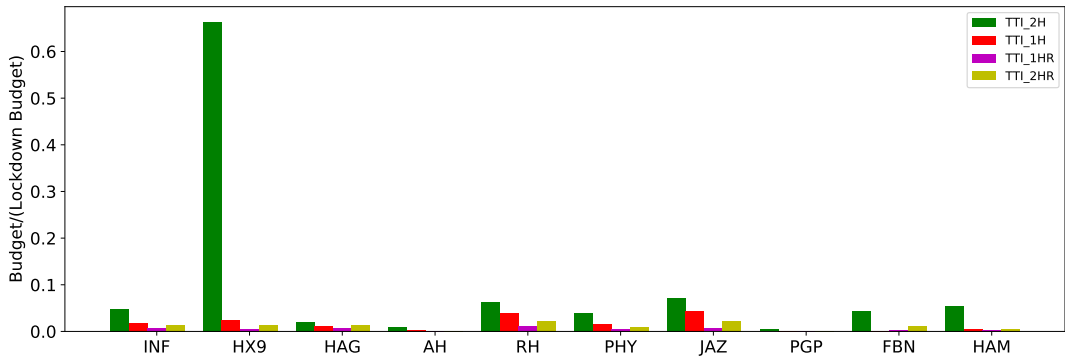

Figure 3: The budget spent on isolation strategies. The budget is normalized by lockdown budget as the baseline. Best viewed in color.

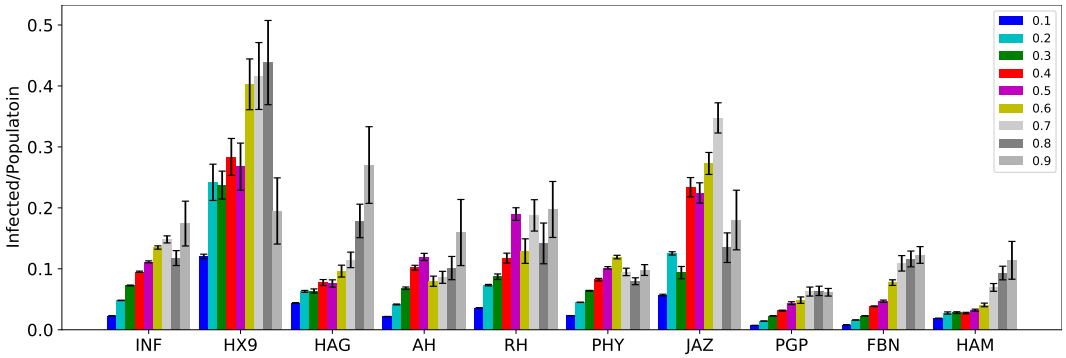

Figure 4: The average proportion of infected individuals over 100 trials of simulation and its variance for different thresholds in CI (community-based isolation strategy). The lower thresholds give considerably better performance than strategies in Figure 2. Best viewed in color.

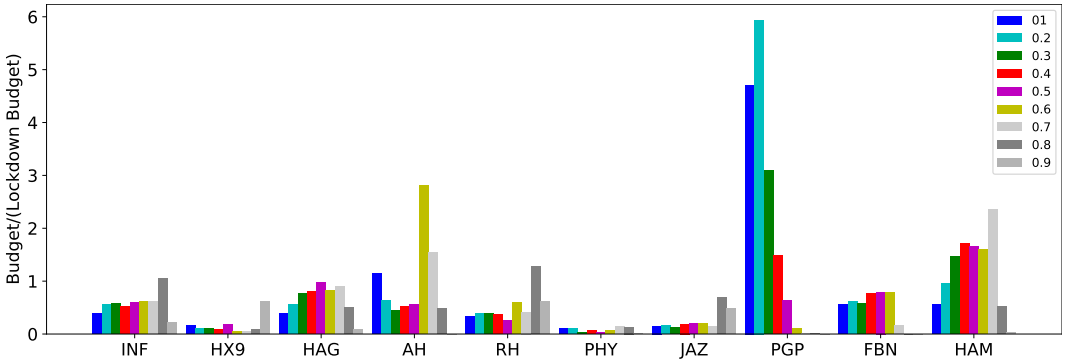

Figure 5: The budget spent on CI for different thresholds. The budget is normalized by lockdown budget as the baseline. Except for PGP, the budget for lower thresholds among all datasets are comparable to those in Figure 3. Best viewed in color.

better than other strategies we discussed in reducing the speed. Our CI strategy only requires the community assignment and the number of infected nodes within the community. This information is readily available through prior knowledge on the individual (e.g., the State or County of residence) and the information on the contagion progress (the [estimate] number of infected individuals). In practice, it is possible to gain more knowledge on the neighborhood of the infected nodes in the community (e.g., through contact-tracing and personal questionnaires upon testing) and use the neighborhood information for targeted isolation.

The special case of PGP. In Figure 5, all datasets follow the same trend that lower (higher) thresholds demand lower (higher) budget, except for PGP. A closer look at PGP community structure reveals large communities with high density (i.e.,

community structure that is considerably close to complete graph structure). In other words, the average path length between nodes in these communities is small and the virus spreads throughout the community much faster than in other datasets. As such, PGP meets the isolation threshold in CI much sooner than the rest of the datasets and forces communities of large size (i.e., containing many nodes) into quarantine. However, the higher speed of spread means higher number of deceased as well. As the CI threshold in Figure 5 grows, it becomes harder for PGP to meet the isolation threshold as many of its members are dead and the CI threshold is defined over the primary size of the community. Hence, less and less communities are put into isolation (the decreased budget in Figure 5) and the peak of infection in Figure 4 matches that of DN in Figure 2. This interesting example shows the limitation of CI in networks with communities that are close to complete graphs. For these type of communities, the 1-hop TTI gives the best trade-off between the peak of infection and budget. However, as is evident from our physical-contact datasets, the real-world human-human contacts have low-density communities and obtain better trade-off using CI strategy.

The choice of community. Throughout this study, we have defined community based on the structural property of the network (e.g., Louvain method). This definition of community expands to real-world communities of people within certain geographical region (e.g., state, county, city) that have more connection within the community than outside. However, there are also attribute-based communities that do not necessarily yield the same structural property. For example, a community defined based on gender, age, and race is not guaranteed to form communities that are dense inside and sparsely connected outwards. Just like communities in online social platforms such as Amazon that do not represent human contact for the modeling purposes of a viral spread, the attribute-based communities may not be a suitable candidate for our proposed community-based mitigation strategy, CI.

The superiority of CI in mitigating the spread shows that designing an optimal community-based strategy for further alleviation of the economic impact is a promising research direction. Moreover, community information can be local and noisy (through individual self-reported or publicly known memberships such as geographical proximity in a region). Our effort is to encourage more research on community-based mitigation strategies rather than brute-force methods such as lockdown or naïve TTI. Although k-hop and community-based methods seem to require extra effort for tracing the impact, they are still practical in real-world. Our results show that with local approximation of network's structure, we still can obtain solutions that reduce both the physical and economic impact of the pandemic in a global scale.

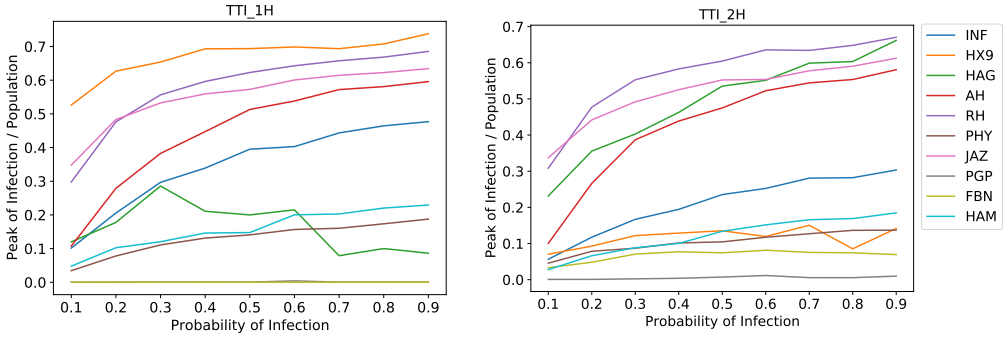

(a) 1-hop Test-Trace-Isolate (b) 2-hop Test-Trace-Isolate

Figure 6: Sensitivity of peak of infection against probability of infection (α). The changes in the value of α affects the datasets in a mostly similar way and does not change our experiment result in Section 4.4. Best viewed in color.

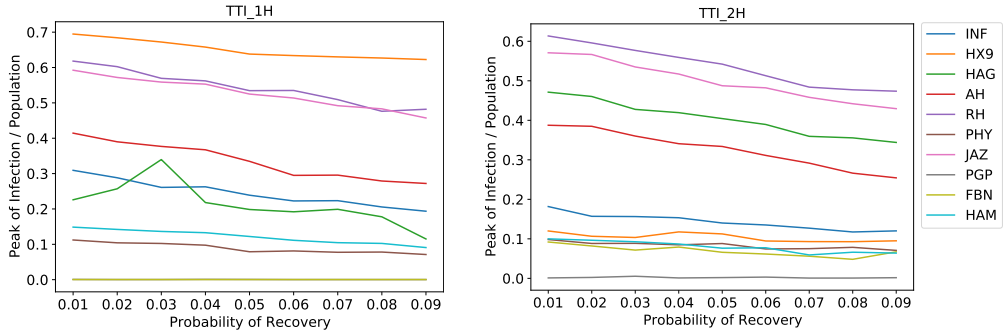

(a) 1-hop Test-Trace-Isolate (b) 2-hop Test-Trace-Isolate

Figure 7: Sensitivity of peak of infection against probability of recovery (β). The changes in the value of β affects the datasets in a mostly similar way and does not change our experiment result in Section 4.4. Best viewed in color.

4.5 Ablation Study

As mentioned in Section 4.3, our choice of hyperparameters in Table 2 does not change the result of our comparative study among different mitigation strategies. Here, we show the robustness of our results against the three degrees of freedom (α, β, and γ) in SIRD model. We repeat the same experiment in Figure 2 for different values of these parameters and report the results on peak of infection for 1-hop and 2-hop Test-Trace-Isolate in Figures 6 to 8. The results for other models were similar and are not included to avoid repetition. As evident from these three figures, the rate of change in peak of infection is mostly similar across all datasets and does not change our comparative observations in Section 4.4.

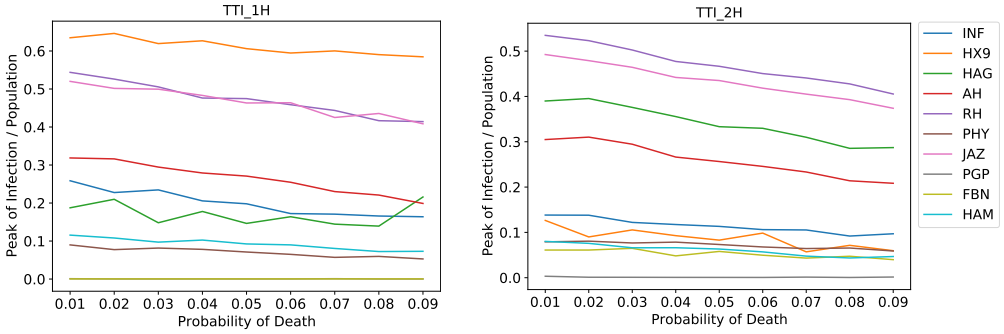

(a) 1-hop Test-Trace-Isolate

(b) 2-hop Test-Trace-Isolate

Figure 8: Sensitivity of peak of infection against probability of death (γ). The changes in the value of γ affects the datasets in a mostly similar way and does not change our experiment result in Section 4.4. Best viewed in color.

5 Conclusion

In this study, we focused on several mitigation strategies practice in real world and provided two strategies that can lead to better performance. We showed (1) The addition of 1-hop neighborhood ranking to TTI can enhance its performance considerably both in cost and reducing the speed of spread, and (2) community membership directly influences the speed of spread with a reasonable cost, and is a promising direction for designing new mitigation strategies. Our results encourage further research on TTI-based and Community-based methods as powerful tools to substitute the current naïve solutions to the pandemic mitigation strategies in early stages.

Future Direction. As discussed earlier, we plan to focus on designing a targeted community-based mitigation algorithm that incorporates local node information as well to reduce the quarantine population (and the cost). This information should be obtainable in practical setting and we count for missing data as well. Another promising direction is to combine our findings on early mitigation strategies with strategies adopted for vaccination in later stages of the contagion. The goal would be to solve an optimization problem that chooses the best vaccination candidates in order to reduce the cost of adopted isolation strategy. For example, vaccinating crucial nodes in a community can lower the community score ($\frac{I_c}{V_c}$) below the isolation threshold T and remove the necessity of isolation that community.

Acknowledgments

This project was supported by Army Research Office award W911NF-18-1-0047.

References

[1] D. Weston, K. Hauck, and R. Amlôt, "Infection prevention behaviour and infectious disease modelling: a review of the literature and recommendations for the future," *BMC public health*, vol. 18, no. 1, p. 336, 2018.

[2] B. J. Cowling, D. M. Ng, D. K. Ip, Q. Liao, W. W. Lam, J. T. Wu, J. T. Lau, S. M. Griffiths, and R. Fielding, "Community psychological and behavioral responses through the first wave of the 2009 influenza a (h1n1) pandemic in hong kong," *The Journal of infectious diseases*, vol. 202, no. 6, pp. 867–876, 2010.

[3] T. Cruwys, M. Stevens, and K. H. Greenaway, "A social identity perspective on covid-19: Health risk is affected by shared group membership," *British Journal of Social Psychology*, 2020.

[4] J. Cannarella and J. A. Spechler, "Epidemiological modeling of online social network dynamics," *arXiv preprint arXiv:1401.4208*, 2014.

[5] T. Kuchler, D. Russel, and J. Stroebel, "The geographic spread of covid-19 correlates with structure of social networks as measured by facebook," tech. rep., National Bureau of Economic Research, 2020.

[6] S. Ma, L. Feng, and C.-H. Lai, "Mechanistic modelling of viral spreading on empirical social network and popularity prediction," *Scientific reports*, vol. 8, no. 1, pp. 1–10, 2018.

[7] P. Holme, "Model versions and fast algorithms for network epidemiology," *arXiv preprint arXiv:1403.1011*, 2014.

[8] T. Britton, "Stochastic epidemic models: a survey," *Mathematical biosciences*, vol. 225, no. 1, pp. 24–35, 2010.

[9] C. Anastassopoulou, L. Russo, A. Tsakris, and C. Siettos, "Data-based analysis, modelling and forecasting of the covid-19 outbreak," *PloS one*, vol. 15, no. 3, p. e0230405, 2020.

[10] E. Bonyah and K. O. Okosun, "Mathematical modeling of zika virus," *Asian Pacific Journal of Tropical Disease*, vol. 6, no. 9, pp. 673–679, 2016.

[11] V. Colizza, A. Barrat, M. Barthelemy, A.-J. Valleron, and A. Vespignani, "Modeling the worldwide spread of pandemic influenza: baseline case and containment interventions," *PLoS Med*, vol. 4, no. 1, p. e13, 2007.

[12] B. Ivorra, M. R. Ferrández, M. Vela-Pérez, and A. Ramos, "Mathematical modeling of the spread of the coronavirus disease 2019 (covid-19) taking into account the undetected infections. the case of china," *Communications in nonlinear science and numerical simulation*, p. 105303, 2020.

[13] Y. B. de Bruin, A.-S. Lequarre, J. McCourt, P. Clevestig, F. Pigazzani, M. Z. Jeddi, C. Colosio, and M. Goulart, "Initial impacts of global risk mitigation measures taken during the combatting of the covid-19 pandemic," *Safety Science*, p. 104773, 2020.

[14] M. I. Meltzer, N. J. Cox, and K. Fukuda, "The economic impact of pandemic influenza in the united states: priorities for intervention.," *Emerging infectious diseases*, vol. 5, no. 5, p. 659, 1999.

[15] A. Atkeson, "What will be the economic impact of covid-19 in the us? rough estimates of disease scenarios," tech. rep., National Bureau of Economic Research, 2020.

[16] B. N. Ashraf, "Economic impact of government interventions during the covid-19 pandemic: International evidence from financial markets," *Journal of Behavioral and Experimental Finance*, vol. 27, p. 100371, 2020.

[17] G. Bonaccorsi, F. Pierri, M. Cinelli, A. Flori, A. Galeazzi, F. Porcelli, A. L. Schmidt, C. M. Valensise, A. Scala, W. Quattrociocchi, *et al.*, "Economic and social consequences of human mobility restrictions under covid-19," *Proceedings of the National Academy of Sciences*, vol. 117, no. 27, pp. 15530–15535, 2020.

[18] C. N. Ngonghala, E. A. Iboi, and A. B. Gumel, "Could masks curtail the post-lockdown resurgence of covid-19 in the us?," *Mathematical biosciences*, vol. 329, p. 108452, 2020.

[19] H. Brüssow, "Covid-19: Test, trace and isolate-new epidemiological data," *Environmental Microbiology*, 2020.

[20] R. S. D. Initiative, "Test, trace, isolate." `http://web.archive.org/web/20080207010024/http://www.808multimedia.com/winnt/kernel.htm`. Accessed: 2020-08-21.

[21] A. Galstyan and P. Cohen, "Cascading dynamics in modular networks," *Physical Review E*, vol. 75, no. 3, p. 036109, 2007.

[22] P. Sah, S. T. Leu, P. C. Cross, P. J. Hudson, and S. Bansal, "Unraveling the disease consequences and mechanisms of modular structure in animal social networks," *Proceedings of the National Academy of Sciences*, vol. 114, no. 16, pp. 4165–4170, 2017.

[23] A. Topîrceanu, "Analyzing the impact of geo-spatial organization of real-world communities on epidemic spreading dynamics," in *International Conference on Complex Networks and Their Applications*, pp. 345–356, Springer, 2020.

[24] M. Salathé and J. H. Jones, "Dynamics and control of diseases in networks with community structure," *PLoS Comput Biol*, vol. 6, no. 4, p. e1000736, 2010.

[25] N. Gupta, A. Singh, and H. Cherifi, "Community-based immunization strategies for epidemic control," in *2015 7th international conference on communication systems and networks (COMSNETS)*, pp. 1–6, IEEE, 2015.

[26] J. Kunegis, "Konect: the koblenz network collection," in *Proceedings of the 22nd International Conference on World Wide Web*, pp. 1343–1350, 2013.

[27] V. D. Blondel, J.-L. Guillaume, R. Lambiotte, and E. Lefebvre, "Fast unfolding of communities in large networks," *Journal of statistical mechanics: theory and experiment*, vol. 2008, no. 10, p. P10008, 2008.